SHAKING TABLE TESTS AND NUMERICAL SIMULATIONS ON SITE-CITY INTERACTION EFFECTS UNDER COMPLEX TERRAINS

Y. Tian[1], X.Z. Lu[2], D.R. Huang[3]

[1] *Ph.D., Key Laboratory of Civil Engineering Safety and Durability of China Education Ministry, Department of Civil Engineering, Tsinghua University, t-y14@tsinghua.org.cn*

[2] *Professor, Key Laboratory of Civil Engineering Safety and Durability of China Education Ministry, Department of Civil Engineering, Tsinghua University, luxz@tsinghua.edu.cn*

[3] *Associate professor, Department of Hydraulic Engineering, Tsinghua University, huangduruo@tsinghua.edu.cn*

Abstract

In densely-populated cities, many structures are constructed close to each other, which significantly affects site characteristics and earthquake wave propagations. Complex site-city interaction (SCI) effects will occur and result in a non-ignorable influence on the input motions to buildings. In addition, observations during historic earthquakes also demonstrated the significance of considering topographic amplification in seismic assessment of buildings located on hilly terrain. Due to its complexity, topographic amplification has not yet been considered in most of the SCI investigations, particularly in experimental tests.

In this study, seven sets of shaking table tests incorporating the complex terrains were conducted. Both of the flat topography and triangular convex topography were modeled using polyurethane foams. Three types of buildings with different heights were assembled using aluminum sheets, aluminum angles, and additional weights. Three building configurations under four input motion excitations were adopted, such that the SCI effects induced by different terrains, buildings, building configurations, and input motions could be investigated.

The test results show that, compared with flat photography, convex topography will cause more complicated SCI effects. The SCI effects on the seismic behavior of buildings on the convex topography is different from that on the flat photography. In general, both the site and the building responses are reduced when the number of buildings increases. However, this also significantly relies on the response spectra characteristics of the input motions. Different input motions may lead to quite different phenomena. Based on the test results, the reliability of a previously proposed numerical coupling scheme for SCI effects simulations is validated.

Then, based on the validated numerical coupling scheme, a parametric analysis of the influence on the site transfer functions by the site-building frequency ratios is conducted. In general, densely-distributed identical buildings will greatly affect the ground motions by restraining frequency components higher than the fundamental frequency of buildings (f_B), and enlarging frequency components lower than f_B. This coincides with the shaking table test findings. This effect will be more significant when the number of buildings increases or when the building and the site frequencies coincide.

Finally, the seismic damage simulation of a virtual community on complex terrains is performed using the numerical coupling scheme. The size of the site considered is 2100 m × 1800 m along the horizontal plane. The height of the site model varies from 230 m to 500 m. 224 buildings on the topography are considered. The case study shows that, as compared with free-field conditions, the response spectra of the input motions to most buildings will show reduced amplitudes for periods shorter than the dominant vibration period of the building, but enlarged amplitudes for longer periods.

In summary, SCI effect has remained a challenging problem to date. In this work, seven sets of shaking table tests of SCI effects considering complex terrains are conducted. The reliability of a previously proposed numerical coupling scheme is validated using the shaking table test results. Through parametric analysis and a case study, SCI effects considering complex terrains are illustrated.

Keywords: Shaking table test, site-city interaction effects, complex terrain, test strategy, numerical coupling scheme

1. Introduction

An earthquake occurring in a densely-populated city may result in severe casualties and economic losses, along with an unacceptable social impact. To prevent and mitigate potential seismic disasters and to improve urban resilience, city-scale nonlinear time-history analysis (NLTHA) of buildings has been widely adopted to simulate urban earthquake scenarios of real cities [1, 2]. In general, free-field ground motions and simplified building models are used to conduct such simulations, so that the characteristics of different ground motions and structures can be considered. The accuracy of the input ground motions is one of the most decisive factors affecting the rationality of the city-scale NLTHA. For a real city, however, large numbers of different types of structures are constructed close to each other, which will lead to significant site-city interaction (SCI) effects, and further affect the site characteristics and earthquake wave propagations. On the other hand, observations during past earthquakes demonstrated the significance of considering topographic amplification in seismic analyses of buildings in mountainous cities, where earthquake waves are amplified at convex terrain features such as hill tops, and are de-amplified at concave features such as valleys [3]. Such site effects along with the extant of buildings, will further complicate the earthquake wave propagations, input motions to buildings and seismic behavior of buildings as compared with free-field conditions [4, 5]. Thus, it is meaningful to research on the SCI effects in mountainous region to understand both of the SCI and topographic amplification effects and their utility in seismic damage assessment of buildings.

To date, there are mainly three research approaches to the SCI effects: theoretical analysis, numerical simulations, and shaking table tests [6, 7, 8, 9, 10]. Because of the complicated scenarios of buildings and corresponding site conditions, an oversimplified theoretical analysis can hardly be applied to real-world earthquake scenarios. Consequently, more researchers prefer using numerical simulation methods in practical SCI effects problems [5, 11]. So far, there have been many shaking table tests and field tests (such as field forced vibration tests and earthquake observations) related to soil-structure interaction (SSI) and structure-soil-structure interaction (SSSI) problems [8, 12, 13, 14]. However, these tests only focus on the interactions between limited numbers of buildings, and cannot sufficiently represent the characteristics of SCI effects [15, 16]. In the shaking table tests for SCI effects, only very small similitude ratios can be adopted, due to the large scale of regions considered. Schwan et al [15] proposed a shaking table test strategy, and performed shaking table tests of SCI effects under different building configurations on flat site models. The results have validated the effectiveness of the proposed strategy.

Despite these convergent observations, it is still uncertain in practice whether a city group-effect can noticeably modify the seismic response of site and buildings, especially for those situated on natural terrain. In particular, the extent up to which the conventional approaches remain efficient is still an open question. This uncertainty may rely on the three following facts. First, the identification of a possible “site-city” effect in the records obtained during earthquake events is a very hard task, due to the uniqueness of each site-city configuration and to the huge amount of information required to discriminate that effect from other complex phenomena. Second, the basic experimental data that would clearly evidence a “site-city” effect is missing: Too few accelerometers are gained during earthquake events (compared to the complexity of the geological site and the city) and, up-to-date, no experiments dealing with multi-structure interactions among a large group of buildings on complex natural terrain have been performed. Third, it is difficult to draw general conclusions or physical rules from the several numerical approaches mentioned above, due to the vast variety of assumptions retained for the building models (single or multiple degrees of freedom), the city model (geometric arrangement, buildings with similar or distinct masses, stiffness, eigenfrequencies), the frequency range of investigation (compared to the buildings and site eigenfrequencies), the nature of the incident wave, and the 2-D or 3-D characteristics of the natural terrain.

Thus, in this work, seven sets of shaking table tests of SCI effects considering complex terrains were designed and performed, adopting different building and site configurations. The test results were further used to validate the numerical coupling scheme proposed by the authors [11]. Then, parametric analysis was conducted by using the validated numerical coupling scheme to study the influence of the site-building frequency ratio on the site transfer functions. Finally, a seismic damage simulation of a virtual community with complex terrains is performed. Simulation results show the influence on the response spectra by the SCI effects, and the importance of nonlinearity of building models.

2. Experimental program

In this test, the test strategy proposed by Schwan et al [15] was adopted: polyurethane foams were used to simulate site models, and aluminum sheets with additional weights were used to simulate buildings [16]. Three types of buildings with different numbers of stories were considered: 3-story (B1), 9-story (B2), and 13-story (B3). According to the similitude ratios by Aldaikh et al [16], the following similitude ratios in Table 1 were adopted in the shaking table tests, using carefully-selected materials.

Table 1 – Similitude ratios of the shaking table test

	Unit	Model	Prototype	Similitude ratio in this work	Similitude ratio by Aldaikh et al [16]
Length	m	0.26	27	1/100	1/100
Shear wave velocity	m/s	44	200	1/4.5	1/4.76
Period (fixed base)	s	0.313	0.9	1/3	1/3
Density	kg/m^3	34.5	2000	1/58	1/26.3

In this test, two types of sites were considered: Site F with a flat topography, and Site H with a triangular convex topography, as shown in Fig.1(a) and Fig.1(b). The polyurethane foam had an elastic modulus of 0.148 MPa, and a density of 34.5 kg/m^3. Each building model consisted of a pair of aluminum angles, one aluminum sheet, and a pair of additional weights (AWs), as shown in Fig.1(c). Two types of AWs were adopted: a pair of aluminum bars (G1), and a pair of steel bars (G2). Each aluminum/steel bar had a size of 1 mm × 20 mm × 1 m. In that regard, the stability of the aluminum sheet under the gravity load limited the maximal height of the assembled building models, considering the very low thickness of the aluminum sheets and the inevitable initial deflections in them. Consequently, three types of building models were considered, as shown in Fig.1(c).

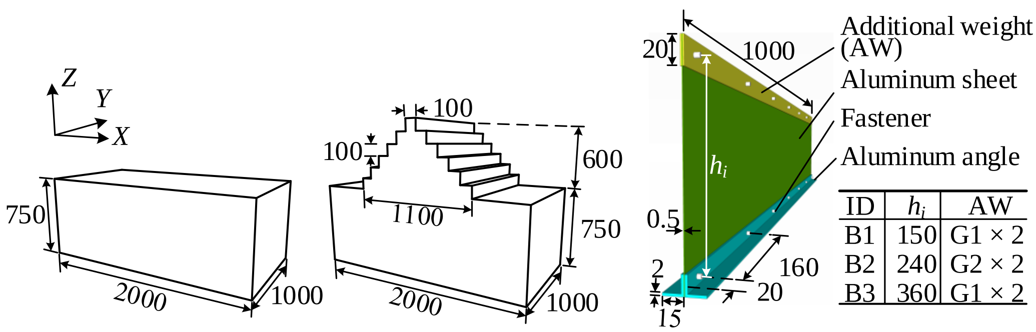

(a) Site F (b) Site H (c) Building model

Fig. 1 – Details of the site and building model (Unit: mm)

Three building configurations were considered: (1) C0: free-field condition without buildings; (2) C1: only one building located at the center of the site, as shown in Fig.2(a); and (3) C2: 17 buildings uniformly distributed on the site with an interval of 0.1 m along the X-axis, as shown in Fig.2(a). Four input motions were applied to the shaking table along the *X*-axis: (1) EQ1: white noise with an amplitude of 1 m/s^2, and a duration of 60 s; (2) EQ2: a Ricker wavelet with a dominant frequency of 8 Hz, peak acceleration of 1 m/s^2, and duration of 2 s; (3) EQ3: El Centro (No. 6 in NGA-West2 Ground Motion Database) [17]. According to the similitude ratios in Table 1, the similitude ratio of acceleration can be determined as 0.09. Thus, the scaled peak acceleration and duration adopted were 0.25 m/s^2 and 17.90 s, respectively; (4) EQ4: Kocaeli (No.1158 in NGA-West2 Ground Motion Database) [17]. The scaled peak acceleration and duration adopted were 0.32 m/s^2 and 9.06 s, respectively.

The building models were small in size and lightweight. Thus, in this test, the ADXL335 Micro Electro Mechanical Systems (MEMS)-based accelerometers [18] were used, owing to their advantages in size and weight. To calibrate the collected data by the ADXL335 accelerometers more accurately, two well-calibrated accelerometers (provided by the Institute of Engineering Mechanics, China Earthquake Administration) were also used to determine the acceleration on the shaking table. Fig.2(b) shows the detailed accelerometer configuration. Here, BP denotes the accelerometer at the top of each building model; SP denotes the accelerometer on the site. The shaking table tests in this work were performed in the laboratory of the Institute of Engineering Mechanics, China Earthquake Administration. The size of the shaking table was 5 m × 5 m, making it easier to shake two site models together. The test results proved that the ADXL335 accelerometers are accurate enough for the purposes of the test, as shown in Fig.2(c).

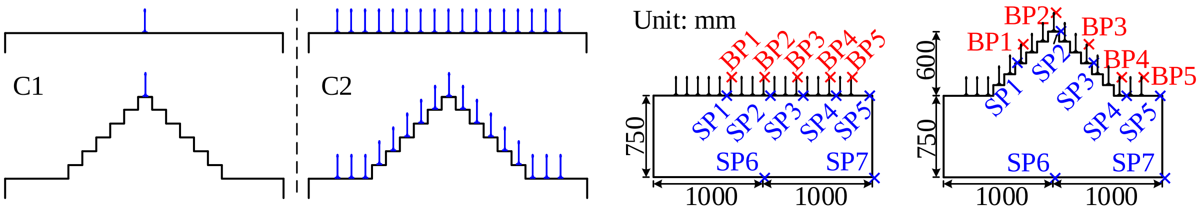

(a) Building configurations (b) Accelerometer configurations

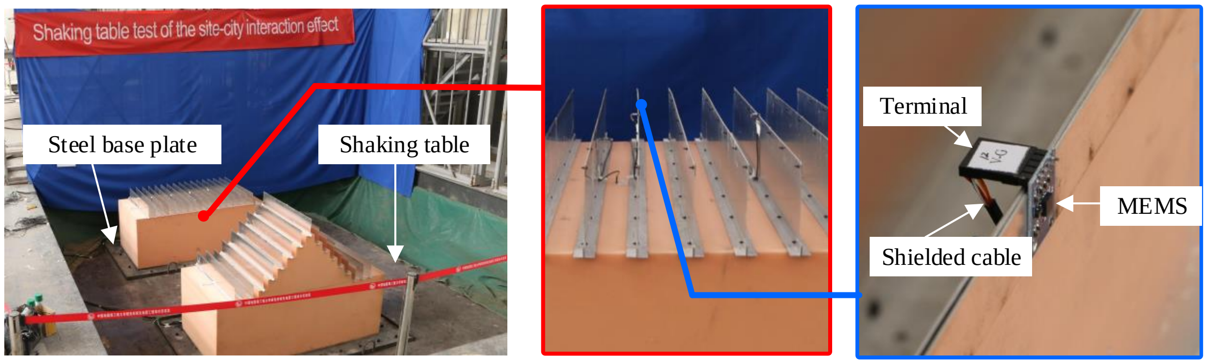

(c) Overview of the test specimens

Fig. 2 – Configurations of building models and accelerometers

3. Test results

Due to the length limit of the paper, only the test results concerned with Building B1 will be discussed. Fig.3 shows the transfer functions for each site at SP2, with respect to the input motions under different load cases. As the number of the buildings increases, the fundamental frequency of each site model (denoted as f_S) will decrease, and the ground motions will be influenced more by the radiated waves from the buildings, leading to a larger perturbation near the fundamental frequency of the buildings (denoted as f_B) in the transfer functions. In the f_B neighborhood, as compared with the free-field conditions, the frequency components greater than f_B will be restrained, whereas the frequency components lower than f_B will be enlarged.

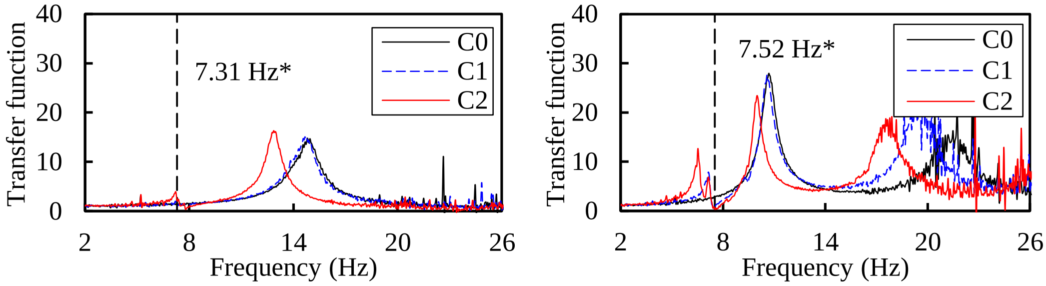

(a) Site F (b) Site H

Fig. 3 – Transfer function results at SP2 with respect to the input motions at the bottom
(*These values are the fundamental frequency of the building at the center of the surface measured at BP2)

Fig.4 provides the normalized peak acceleration at SP1 to SP5 of both sites (Site F and Site H) under different excitations. The peak acceleration records are normalized by the peak acceleration recorded at SP2 under the F-C0 condition. Details regarding the positions of SP1 to SP5 are illustrated in Fig.2(b).

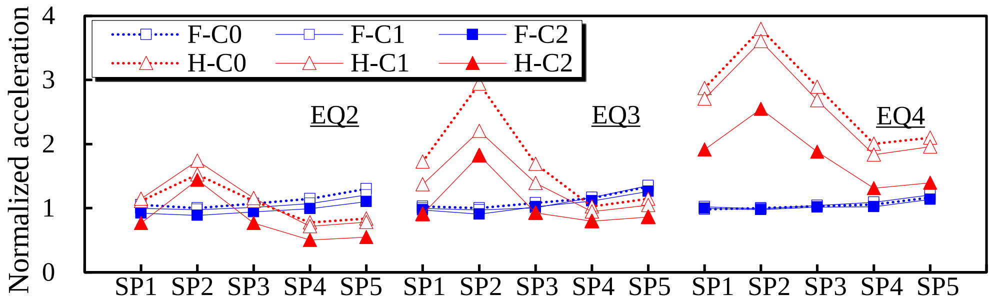

Fig. 4 – Normalized peak accelerations at SP1 to SP5

Under the same building configurations, the top of Site H shows larger amplification effects than those in Site F, whereas the foot of the convex topography on Site H shows a smaller peak acceleration as compared with that of Site F. The test results under the EQ4 excitations are relatively special, owing to the response spectrum characteristics of EQ4. The response spectrum of EQ4 at *f*s of Site F is small, whereas the response spectrum at *f*s of Site H is large. In addition, according to the response spectrum of EQ4, Site F will show larger responses when applying any measurement that can reduce the fundamental frequency of Site F (such as using building configuration C2, or adding an additional convex topography as Site H). These results illustrate that the SCI effects are influenced not only by building and site characteristics, but also by the input motions.

For Site F, the input motions for buildings will be reduced when the number of buildings increases. Nevertheless, this change still depends on specific input excitations. For Site H, its fundamental frequency is generally situated at the descending part of the response spectra of the input motions. Thus, the response of Site H and the corresponding input motions for buildings will be reduced as the number of buildings increases. However, when there is only one building on the top of Site H, more weight is concentrated on the top, leading to significantly amplified responses. In general, Site H (with the convex topography) will show more complex SCI effects as compared with Site F.

Fig.5 provides the normalized peak acceleration at BP1 to BP5 of both sites (Site F and Site H) under different excitations. The peak acceleration records are normalized by the peak acceleration recorded at BP2 under the F-C1 condition.

In general, the responses of buildings are basically proportional to the input motion intensity. The buildings on the top of Site H deform the most, whereas the buildings on the foot of the convex topography on Site H show the smallest responses. When the number of buildings increases, the responses at BP2 on Site F vary little, whereas the responses at BP2 on Site H will decrease.

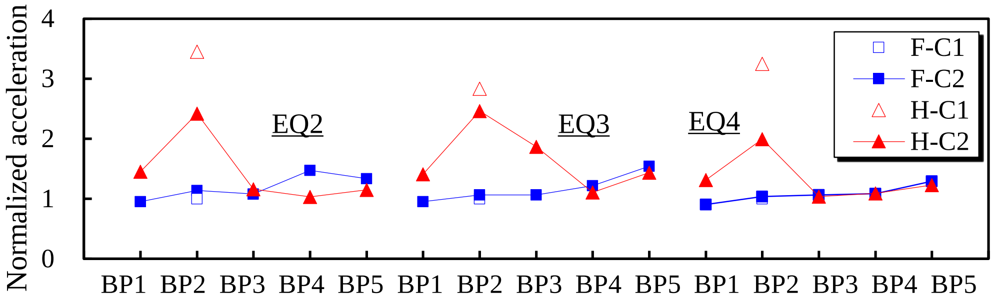

Fig. 5 – Normalized acceleration responses at BP1 to BP5

4. Simulation of test results and parametric analysis

Lu et al [11] proposed a numerical coupling scheme for SCI effects simulation based on nonlinear MDOF building models and spectral element soil models (provided by the open sourced software SPEED [9]). This numerical coupling scheme has been open-sourced at the following URL: https://github.com/research-group-of-Xinzheng-Lu/SCI-effects-simulation. This method has been validated through existing shaking table tests in literature. To further illustrate the reliability of this method, this section will use this numerical scheme to simulate the shaking table tests reported in this work. The detailed modeling method can be found in [11].

Part of simulation results for load cases containing B1 under the EQ2 excitation are shown and compared with the test results in Fig.6. The comparison results show good agreement between the simulation results and test data. In terms of the transfer functions, the proposed numerical coupling scheme can determine the characteristics of SCI effects on ground motion propagations, and the perturbation features in the f_B neighborhood coincide with the test results.

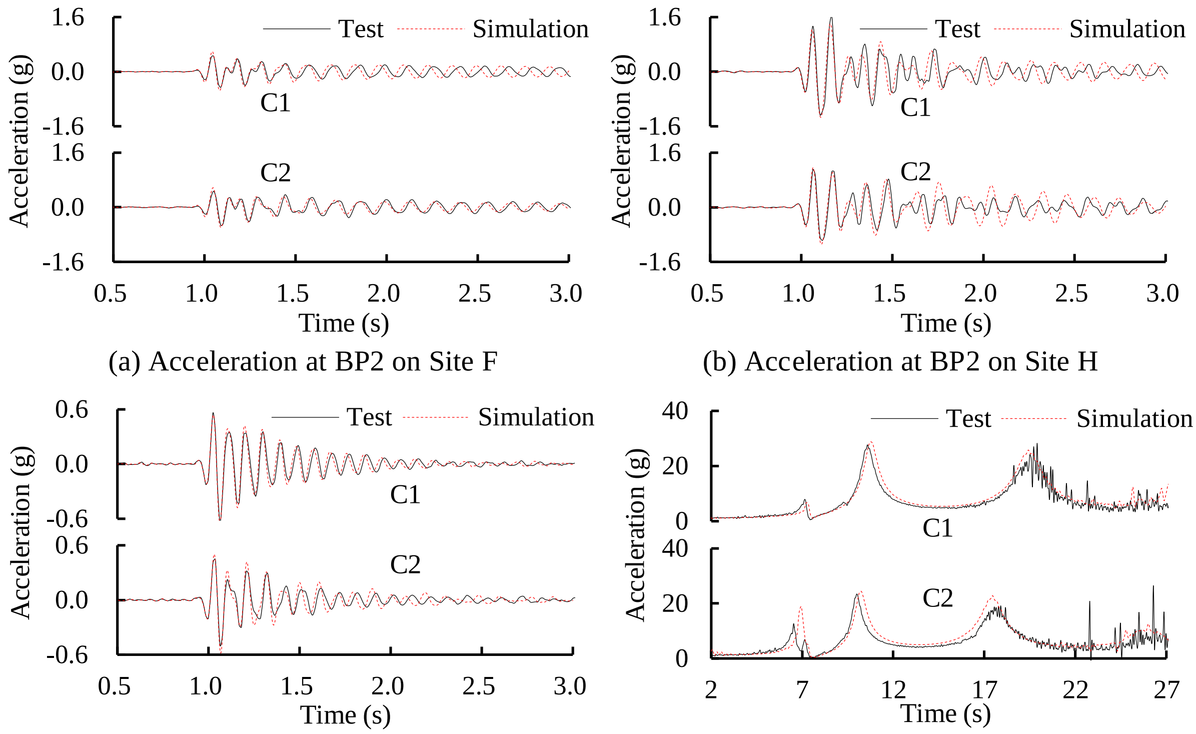

(a) Acceleration at BP2 on Site F
(b) Acceleration at BP2 on Site H
(c) Acceleration at SP2 on Site H
(d) Transfer function at SP2 on Site H

Fig. 6 – Comparison between simulation and test results

Test results in Section 3 illustrate that the site transfer functions will show apparent perturbation features near the fundamental frequency of the buildings (f_B). Thus, to furthur study this perturbation features, this section will conduct a parametric analysis by varying the site-building frequency ratio (f_S/f_B). Specifically, this section obtains values of f_S/f_B at 0.2, 0.4, 0.6, 0.8, 1.0, 1.2, 1.4, 1.6, 1.8, 2.0, and 5.0 by adjusting the f_B alone, while keeping f_S and the other building parameters identical to the shaking table test. Through the parametric analysis, Fig.7 shows the transfer functions at SP2 with respect to the input motions under different site-building frequency ratios. In Fig.7, each colored arrow shows the f_B value used in each case. The transfer function curve of the corresponding case has the same color. Different numbers represent the results under different site-building frequency ratios (where SCI effects are considered). FF denotes the results under free-field conditions; FF-FM means that the buildings are not considered, but the masses of the building foundations are considered. The results illustrate that the SCI effects on the transfer functions become the most significant when the building and site frequency coincide, and that the frequency components in the f_B neighborhood will be restrained the most.

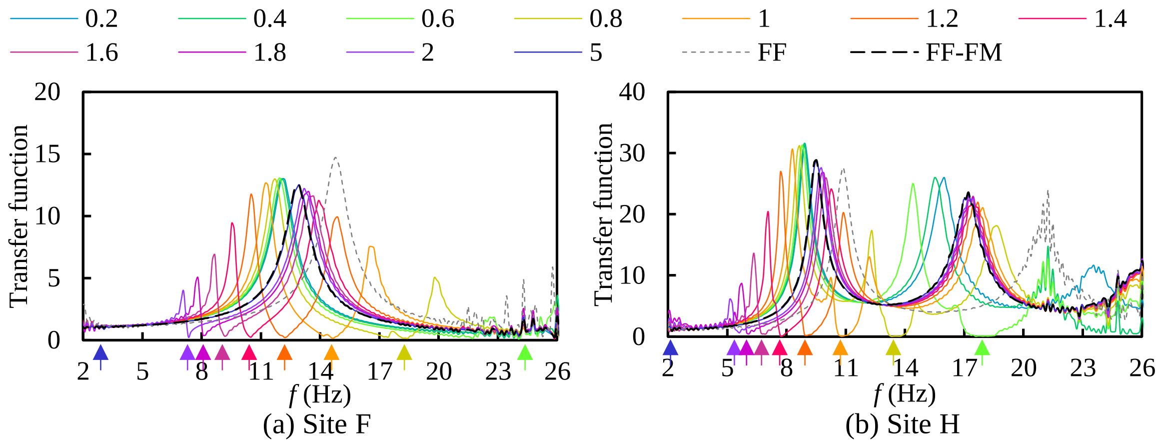

Fig. 7 – Transfer function comparison among cases with different frequency ratios

Specifically, because of the existence of the building foundation mass, the fundamental frequency of the site will be reduced (FF-FM) as compared to the free-field conditions (FF). Based on FF-FM, the existence of buildings will further change the transfer functions of the site. For Site F, when the site-building frequency ratio is large ($f_S/f_B \geq 5$), meaning that the building frequency is low, the site exhibits a single vibration mode. Conclusively, if the building frequency is far below the frequency of the site, the influence by the reaction force from the building on the site is negligible. When f_B approaches f_S, the frequency components near f_B will be significantly restrained, leading to two main peaks in the transfer functions. In terms of Site H, similar phenomena can be found. However, the results for Site H are more complex, owing to the existence of the convex topography.

5. Case study of a virtual community on complex terrains

To further illustrate the SCI effects under complex terrains, a virtual community is adopted as a case study. Here, the terrains and building distributions in the established numerical model are very close to the real scenarios, and are based on an available digital elevation model (DEM) and map data. The building information (such as building height and the number of stories) is obtained through site investigation. In this case, the size of the site considered is 2100 m × 1800 m ($X \times Y$) along the horizontal plane. The height of the site model varies from 230 m to 500 m, as shown in Fig.8(a). 224 buildings are considered, as shown in Fig.8(b). The foundations of the buildings are not considered because of the low height of the buildings. The design intensity of the buildings is assumed as 8-degree specified in the Chinese seismic design code (with a peak ground acceleration (PGA) of 0.20 g at a 10% probability of exceedance at the 50-year hazard level) [19].

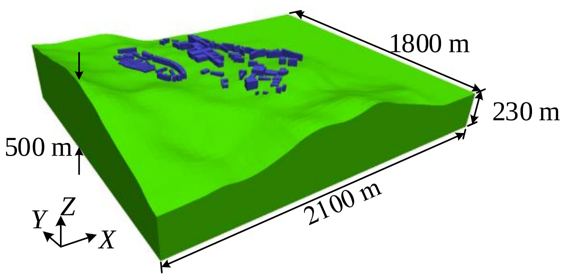

(a) Global view of the model

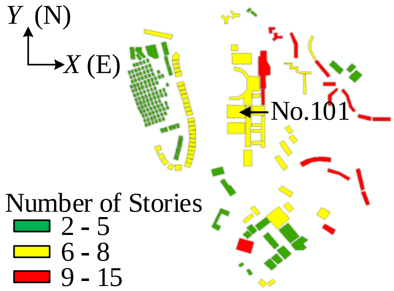

(b) Distribution of number of stories

Fig. 8 – Virtual community model for site-city interaction (SCI) simulation

In the virtual community, the western part of the site (negative *X*-axis direction) is covered with densely-distributed low-story buildings, whereas the buildings on the eastern part (positive *X*-axis direction) are relatively tall. According to Guo et al [20] and Wang et al [3], the shear velocity for the first 20 m-depth soil layer is set as 300 m/s, and the remaining part is set as rock, with a shear velocity of 1000 m/s. The density of the soil is set as 2000 kg/m^3. Two load cases are considered:

(1) Case V1: the earthquake wave propagation in the site is simulated under a free-field condition, and the building responses are simulated based on the free-field motions; and

(2) Case V2: the SCI effects are considered during the computation, using the proposed numerical coupling scheme by Lu et al [11].

In Cases V1 and V2, both elastic building models (denoted as Cases V1E and V2E) and nonlinear building models (denoted as Cases V1N and V2N) are adopted. The parameters of the MDOF models of the elastic and nonlinear building models are determined according to the method proposed by Xiong et al [21].

In addition, the El Centro record [17] is adopted as the target rock outcropping motion. Then, the SHAKE program [22] is used to perform the deconvolution of the input motion at the bottom of the site. The deconvoluted motion is applied to the bottom of the site as the vertical input motion along the *X*-axis. The absorbing boundary is adopted.

Fig.9 shows the PGA amplification ratios of Case V2 with respect to Case V1 ($PGA_{CaseV2}/PGA_{CaseV1}$ - 1). The PGA amplification ratios show that most of the PGAs at the building positions will decrease when the SCI effects are considered. The largest reduction can exceed 20%. The cases using elastic and nonlinear building models generally show similar PGA amplification ratio distributions.

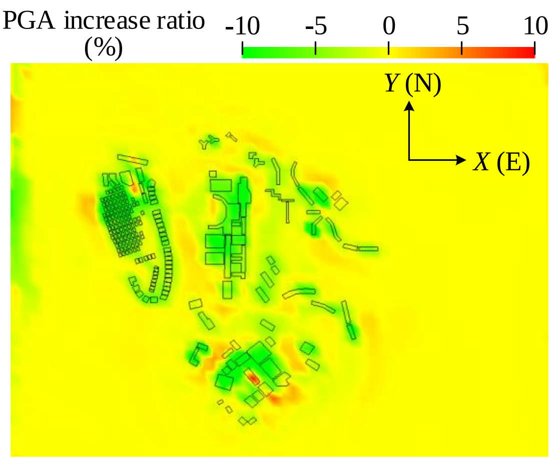

(a) Case V1E & V2E (Elastic building model)

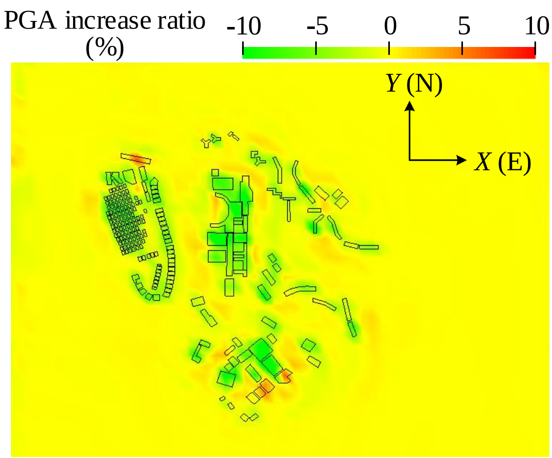

(b) Case V1N & V2N (Nonlinear building model)

Fig. 9 – Ground motion intensity increase ratio distribution

Fig.10 shows the seismic responses of buildings in Case V2 as compared with the free-field conditions (Case V1). The results show that for each building, the change of the peak roof drift ratio (PRDR) is similar to that of the peak inter-story drift ratio (PIDR). When elastic building models are adopted, the PIDR increase ratios and PRDR increase ratios vary from -24.0% to 4.9% and from -25.8% to 9.4%, respectively. When nonlinear building models are adopted, the PIDR increase ratios and PRDR increase ratios vary from -9.4% to 1.7% and from -9.1% to 8.5%, respectively.

Further analysis shows that more than 80% of the buildings exhibit smaller dynamic responses when the SCI effects are considered, for both elastic and nonlinear building model cases. Although the rest of the buildings show increased responses when SCI effects are considered, their PRDR and PIDR increase ratios are small.

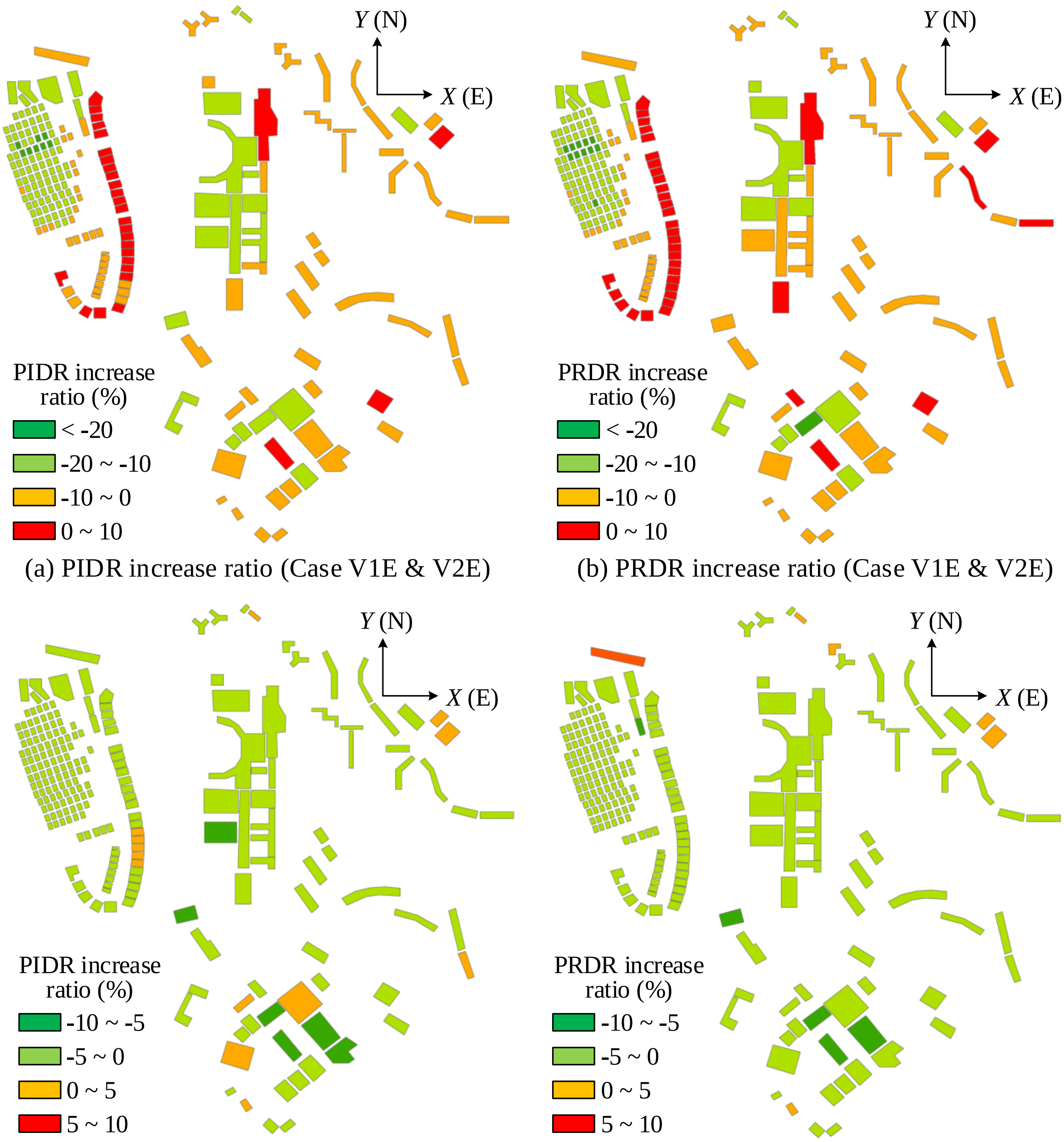

(a) PIDR increase ratio (Case V1E & V2E) (b) PRDR increase ratio (Case V1E & V2E)

(c) PIDR increase ratio (Case V1N & V2N) (d) PRDR increase ratio (Case V1N & V2N)

Fig. 10 – Seismic response increase ratio distribution

The response of Building No. 101 is analyzed in detail as an example. The position of Building No. 101 is shown in Fig.8. It is a 7-story reinforced concrete frame structure. Fig.11 shows the input ground motions and the roof displacements in different cases. The elastic fundamental period of Building No. 101 is 0.7 s. When the building enters the nonlinear stage, the dominant frequency caused by the nonlinear behavior is approximately 1.1 s (as shown in Fig.11(b)), which can be obtained through spectral analysis.

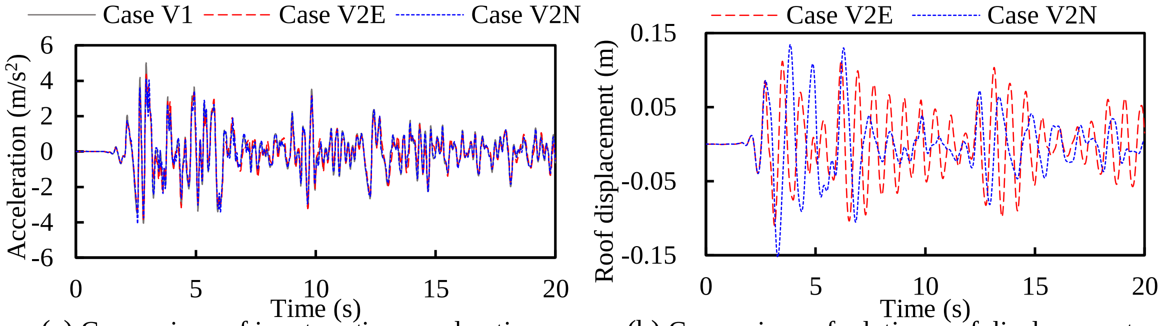

(a) Comparison of input motion acceleration (b) Comparison of relative roof displacement

Fig. 11 – Comparison of the input motion acceleration and relative roof displacement

Fig.12(a) shows the response spectra of the input ground motion in different cases. Fig.12(b) shows the ratio between the response spectra obtained from Case V2 and Case V1. When the SCI effects are considered, the corresponding response spectra show reduced amplitudes for periods shorter than the dominant vibration period, and enlarged amplitudes for longer periods. This phenomenon is similar to the SCI effects on the transfer functions, as discussed in Sections 3 and 4.

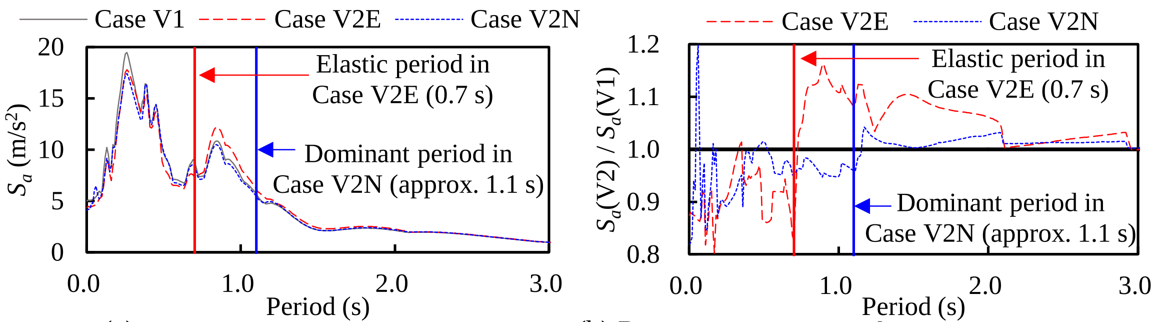

(a) Input motion response spectra (b) Response spectra ratio between Cases V2 & V1

Fig. 12 – Comparison of input motion response spectra

6. Conclusions

In this work, seven sets of shaking table tests of SCI effects considering complex terrains are conducted. The reliability of a proposed numerical coupling scheme is validated using the shaking table test results. Through parametric analysis and a case study, SCI effects are illustrated while considering complex terrains. The following conclusions can be drawn.

(1) Densely-distributed buildings will greatly affect the site characteristics. In the neighborhood range of the fundamental frequency of each building f_B, as compared with free-field conditions, the transfer function amplitude will decrease for frequency components higher than f_B, and will increase for frequency components lower than f_B.

(2) In general, the amplitude of the input motion to buildings will decrease when the number of buildings increases. However, this feature still relies on specific earthquake wave and site characteristics. Terrains will complicate the ground motion distribution.

(3) The proposed numerical coupling scheme can accurately obtain the characteristics of the SCI effects. The case study shows that, as compared with free-field conditions, the response spectra of the input motion show reduced amplitudes for periods shorter than the dominant vibration period of the building, and enlarged amplitudes for longer periods.

(4) For identical site and building configurations, the use of elastic and nonlinear building models will lead to different results. Thus, it is important to consider the building nonlinearity in such a simulation.

7. Acknowledgements

The authors would like to acknowledge the financial supports of the National Natural Science Foundation of China (No. 51778341). The authors would also like to thank for the support of the staff and technicians of the Institute of Engineering Mechanics, CEA, and the postgraduates of Tsinghua University.

8. References

[1] Hori M (2006): *Introduction to Computational Earthquake Engineering*. Imperial College Press, London.

[2] Lu XZ, Guan H (2017): *Earthquake Disaster Simulation of Civil Infrastructures: From Tall Buildings to Urban Areas*. Springer, Singapore.

[3] Wang G, Du CY, Huang DR, Jin F, Koo RCH, Kwan JSH (2018): Parametric models for 3D topographic amplification of ground motions considering subsurface soils. *Soil Dynamics and Earthquake Engineering*, **115**, 41-54.

[4] Guidotti R, Mazzieri I, Stupazzini M, Dagna P (2012): 3D numerical simulation of the site-city interaction during the 22 February 2011 MW 6.2 Christchurch earthquake. *15th World Conference of Earthquake Engineering*, Lisboa, Portugal.

[5] Isbiliroglu Y, Taborda R, Bielak J (2015): Coupled soil-structure interaction effects of building clusters during earthquakes. *Earthquake Spectra*, **31** (1), 463-500.

[6] Boutin C, Roussillon P (2004): Assessment of the Urbanization Effect on Seismic Response. Bulletin of the *Seismological Society of America*, **94** (1), 251-268.

[7] Bard PY, Chazelas J, Guéguen P, Kham M, Semblat JF (2006): Site-City Interaction. In: *Assessing and Managing Earthquake Risk*. Springer, Dordrecht, pp 91-114.

[8] Lou M, Wang H, Chen X, Zhai YM (2011): Structure-soil-structure interaction: literature review. *Soil Dynamics and Earthquake Engineering*, **31** (12), 1724-1731.

[9] Mazzieri I, Stupazzini M, Guidotti R, Smerzini C (2013): SPEED: SPectral Elements in Elastodynamics with Discontinuous Galerkin: a non-conforming approach for 3D multi-scale problems. *International Journal for Numerical Methods in Engineering*, **95** (12), 991-1010.

[10] Kato B, Wang G (2019): Fully Integrated 3D Analysis on Site-City Interaction in an Urban Transport Hub. *ASCE Geotechnical Special Publication GSP 304, International Conference on Geotechnical and Earthquake Engineering 2018 (IACGE 2018)*, Chongqing, China.

[11] Lu XZ, Tian Y, Wang G, Huang DR (2018): A numerical coupling scheme for nonlinear time-history analysis of buildings on a regional scale considering site-city interaction effects. *Earthquake Engineering & Structural Dynamics*, **47** (13), 2708-2725.

[12] Maccalden PB (1969): *Transmission of Steady-state Vibrations between Rigid Circular Foundations*. Dissertation, University of California.

[13] Mizuno H (1980): Effects of structure-soil-structure interaction during various excitations. *7th World Conference of Earthquake Engineering*, Istanbul, Turkey.

[14] Nakagawa S, Kuno M, Naito Y, Nozawa T, Momma T, Mizuno J, Tsukamoto T, Motohashi S, Niwa M (1998): Forced vibration tests and simulation analyses of a nuclear reactor building. *Nuclear Engineering and Design*, **179** (2), 145-156.

[15] Schwan L, Boutin C, Padrón LA, Dietz MS, Bard PY, Taylor C (2016): Site-city interaction: theoretical, numerical and experimental crossed-analysis. *Geophysical Journal International*, **205** (2), 1006-1031.

[16] Aldaikh H, Alexander NA, Ibraim E, Knappett J (2016): Shake table testing of the dynamic interaction between two and three adjacent buildings (SSSI). *Soil Dynamics and Earthquake Engineering*, **89**, 219-232.

[17] Chiou B, Darragh R, Gregor N, Silva W (2008): NGA Project Strong-Motion Database. *Earthquake Spectra*, **24** (1), 23-44.

[18] Bhattacharya S, Krishna AM, Lombardi D, Crewe A, Alexander NA (2012): Economic MEMS based 3-axis water proof accelerometer for dynamic geo-engineering applications. *Soil Dynamics and Earthquake Engineering*, **36**, 111-118.

[19] GB50011-2010 (2010): *Code for Seismic Design of Buildings (GB50011-2010)*. China Architecture & Building Press, Beijing.

[20] Guo X, Wong YL, Yuan YF (2000): Preliminary study on site classification for Hong Kong. *World Information on Earthquake Engineering*, **16** (1), 51-60.

[21] Xiong C, Lu XZ, Lin XC, Xu Z, Ye LP (2017): Parameter determination and damage assessment for THA-based regional seismic damage prediction of multi-story buildings. *Journal of Earthquake Engineering*, **21** (3), 461-485.

[22] Schnabel PB, Lysmer J, Seed HB (1972): SHAKE: a computer program for earthquake response analysis of horizontal layered sites. *Earthquake Engineering Research Center (EERC) Report*, University of California at Berkeley.

